Domino reaction between 2-acylfurans and diethyl azodicarboxylate: a combined experimental, theoretical, X-ray and dynamic NMR study

M. Eugenia González-Rosende,[a] José Sepúlveda-Arques,*[a] Elena Zaballos-Garcia,[a] Luis R. Domingo,*[b] Ramón J. Zaragozá,[b] W. Brian Jennings,*[c] Simon E. Lawrence[c]† and Donal O'Leary[c]

[a] *Department of Organic Chemistry, Faculty of Pharmacy, University of Valencia, Burjassot, Spain*
[b] *Department of Organic Chemistry, Faculty of Chemistry, University of Valencia, Burjassot, Spain*
[c] *Department of Chemistry, University College Cork, Cork, Ireland*

Received (in Cambridge) 24th August 1998, Accepted 30th October 1998

Treatment of 2-acetylfuran **6a** with diethyl azodicarboxylate gave the cycloadduct **7**, 6,7-diethoxycarbonyl-6,7-diaza-8-oxabicyclo[3.2.1]oct-3-en-2-one, whereas 5-methyl-2-formylfuran **6b** reacted giving a simple hydrazide product derived from radical reaction on the formyl group. The structure of the bicyclic compound **7**, established by NMR measurements, was confirmed by an X-ray crystallographic analysis. Variable temperature ^{1}H NMR and ^{13}C NMR studies of **7** indicate that this compound undergoes two distinct dynamic conformational changes with $\Delta G^{\ddagger}$ 10.2 and 13.1 kcal mol^{-1} respectively. The reaction mechanism associated with the domino reaction between furfural **1** and dimethyl azodicarboxylate **9** to give the cycloadduct **10** has been theoretically characterized using *ab initio* methods at the RHF/6-31G* level. The reaction pathway can be described as a three-step process. The first step corresponds with a [4 + 2] cycloaddition between **1** and **9**, while the two subsequent steps are associated with a structural isomerization of the initial formyl cycloadduct to a more stable final adduct.

Introduction

Our previous investigations[1] into the reactivity of heterocyclic formyl derivatives have shown that the reaction of 2-formylfuran (furfural) **1** with diethyl azodicarboxylate (DEAZD) gives an unexpected adduct believed to have the unusual [3.2.1]-bicyclic structure **2**. In contrast, 2-formylthiophene and 2-formylpyrroles **3** react with DEAZD to give simple products **4** and **5** derived from radical reactions on the formyl group (Scheme 1).[1,2] This illustrates the different reactivity of the

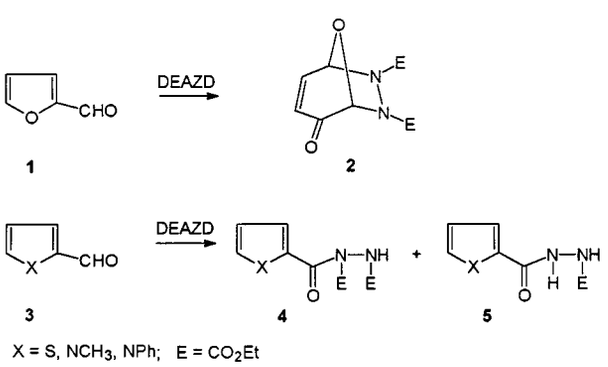

Scheme 1

furan ring in comparison with thiophene and pyrrole.[3] Furan can undergo Diels–Alder cycloadditions but normally an activated dienophile is necessary. The reactivity of the furan ring is considerably enhanced by the presence of an electron-donating substituent at the 2-position and further reduced by electron-withdrawing substituents.[3,4]

It was tentatively suggested that the bicyclic adduct **2** might have been formed by an initial Diels–Alder cycloaddition between furfural and DEAZD, followed by two 1,3-dipolar processes (Scheme 2).[1] This unexpected result prompted us to

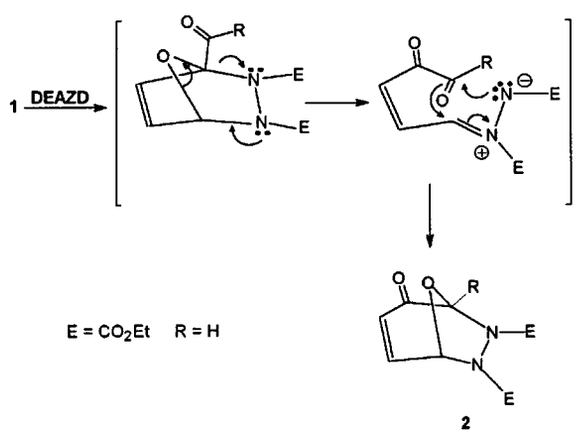

Scheme 2

study the reaction of other acylfurans **6a** (R = CH_3, R′ = H), **6b** (R = H, R′ = CH_3) and **6c** (R = CH_3, R′ = CH_3) with DEAZD under similar conditions (Scheme 3). A dynamic NMR study of the new diazabicyclic compound **7**, also characterized by X-ray structural analysis, is reported. The reaction mechanism associated with the domino reaction between furfural **1** and dimethyl azodicarboxylate **9** as a model is theoretically characterized using *ab initio* MO methods.

† Corresponding author for X-ray crystallography.

Table 1 Comparison of ^{1}H NMR data for compounds **7** and **2**

	Compound **7**[a]		Compound **2**[b]	
Signal	δ	*J*/Hz	δ	*J*/Hz
CH_2CH_3	1.20	7.1 (t)	1.22	7.1 (t)
CH_2CH_3	1.32	7.1 (t)	1.33	7.1 (t)
1-CH_3	1.73	— (s)	—	—
OCH_2	4.14	7.1 (m)	4.15	7.1 (m)
OCH_2	4.29	7.1 (q)	4.29	7.1 (m)
C3-H	6.03	9.8 (d)	6.06	9.9 (d)
C5-H	6.26	4.0 (d)	6.36	4.0 (d)
C4-H	7.02	4.0, 9.8 (dd)	7.10	4.0, 9.9 (dd)

[a] In CD_2Cl_2 solution at 20 °C. [b] In CD_2Cl_2 solution at −10 °C (where signals were well resolved).

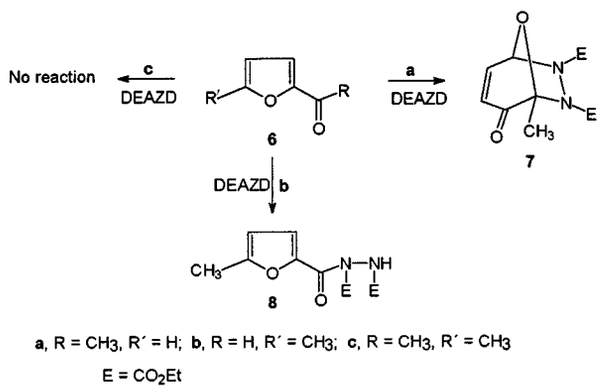

a, R = CH_3, R′ = H; b, R = H, R′ = CH_3; c, R = CH_3, R′ = CH_3

E = CO_2Et

Scheme 3

Results and discussion

Reaction products

Reaction of 2-acetylfuran **6a** with excess DEAZD in a sealed tube at 70 °C gave a crystalline adduct **7**, mp 63–65 °C. The ^{1}H NMR spectrum of this adduct establishes that it has the same 6,7-diaza-8-oxabicyclo[3.2.1]oct-3-en-2-one skeleton as a previously reported product (**2**) from furfural.[1] The signal positions and coupling constants for adduct **7** are remarkably similar to those for compound **2** except that the C1–H signal in **2** is replaced by a methyl signal in **7** (Table 1). In particular the chemical shifts of C3–H (δ 6.03) and C4–H (δ 7.02) and their mutual 9.8 Hz coupling constant, together with the 4.0 Hz vicinal coupling between C4–H and C5–H (δ 6.26), supports the *cis*-enone bridge structure in **7**. The ^{13}C signal positions, assigned with the aid of two-dimensional ^{1}H–^{13}C HETCOR spectra, also support the proposed structure. Thus, the ring carbons gave signals in expected regions *viz*: δ 94.7 (C1), 188.9 (C2), 127.0 (C3), 141.4 (C4) and 84.0 (C5) and the substituent carbons gave signals at δ ($CDCl_3$) 16.6 (C-1 methyl), 14.0 and 14.1 (ester CH_3), 62.8 and 63.9 (ester OCH_2), and 155.0 and 157.3 (ester CO_2). In contrast with spectra of **2**, compound **7** exhibited no detectable line broadening in the ^{1}H and ^{13}C NMR spectra recorded at ambient temperature.

Surprisingly, the reaction of 2-formyl-5-methylfuran **6b** with DEAZD under similar conditions afforded exclusively the furyl diethoxycarbonylhydrazide **8**. No evidence of a bicyclic adduct was found in ^{1}H NMR spectra of the crude reaction product. The ^{1}H NMR spectrum of **8** showed two doublets at δ ($CDCl_3$) 6.07 and 7.08 with a coupling constant of 3.3 Hz characteristic of vicinal protons in a 2,5-disubstituted furan ring, and the ^{13}C NMR showed furan ring signals at δ ($CDCl_3$) 108.7 (CH), 121.4 (CH), 144.4 (C) and 153.2 (C) plus three carbonyl signals at δ 155.2, 155.6 and 157.4. Compound **8** also gave a parent MH^+ ion at *m/z* 285.1088 (CI-MS) consistent with the molecular formula $C_{12}H_{16}N_2O_6$. This hydrazide product is formed by a free-radical reaction at the formyl group.[5]

Table 2 Selected X-ray bond angles and torsion angles for **7**

C1–N7–N6	110.1(6)°	O10–C2–C3–C4	−166.7(10)°
C1–N7–C16	123.4(7)°	C9–C1–C2–O10	9.1(13)°
N6–N7–C16	115.9(6)°	C5–N6–N7–C1	16.3(10)°
C5–N6–N7	101.3(7)°	C11–N6–N7–C16	103.9(10)°
C5–N6–C11	116.3(8)°	N7–N6–C11–O15	−24.5(13)°
N7–N6–C11	115.0(9)°	N6–N7–C16–O20	−15.8(17)°
C1–C2–C3–C4	10.9(13)°	N7–N6–C11–O12	163.0(7)°
C2–C3–C4–C5	−0.4(14)°	N6–N7–C16–O17	167.5(8)°

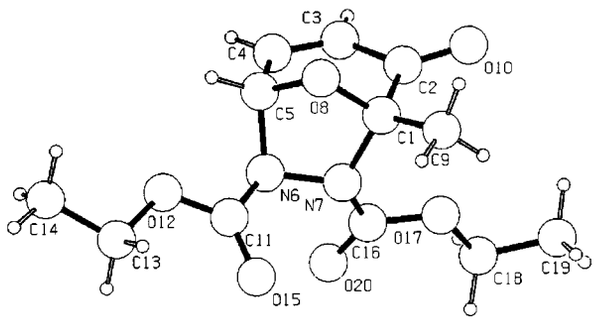

Fig. 1 X-Ray molecular structure of cycloadduct **7**.

Attempted reaction of 2-acetyl-5-methylfuran (**6c**) with DEAZD under similar conditions afforded mainly recovered starting material accompanied by polymeric byproducts. The bicyclic adduct was not detected in ^{1}H NMR spectra of the crude reaction product.

X-Ray crystal structure

Considerable difficulty was experienced in obtaining good quality diffraction results on cycloadduct **7** due to poor scattering and crystal deterioration during data collection. The best of several attempts gave 944 unique reflections for a crystal in the chiral space group $P2_12_12_1$. The data were refined isotropically to an *R*-value of *ca.* 7%. The resulting structure (Fig. 1) confirms the proposed [3.2.1]-bicyclic hydrazide structure for adduct **7**. The hydrazide bridge is twisted by 16° as determined from the C5–N6–N7–C1 torsion angle (Table 2). The alkene portion of the enone bridge is planar, but the bridge is somewhat twisted in the vicinity of the carbonyl group with C1–C2–C3–C4 and O10–C2–C3–C4 torsion angles of 11 and 167° respectively (Table 2) compared with 0 and 180° respectively for a fully coplanar bridge. The most unexpected aspect of the structure is the marked difference in geometry at the two nitrogen atoms. Thus N6 is highly pyramidal with the sum of the three bond angles at this nitrogen (ΣN6) equal to 333° whereas the other nitrogen atom is considerably flattened (ΣN7 = 349°). A planar, or near planar, nitrogen sp^2 hybrid geometry is expected for carbamate systems as conjugation with the carbonyl groups is maximised when the nitrogen lone pair is in a p-orbital. Hence, acyclic and six-membered cyclic 1,2-dialkoxycarbonylhydrazines normally have ΣN close to 360°.[6] A longer N6–C11 carbamate bond compared with N7–C16 might be expected, due to a reduced conjugative interaction of the pyramidal N6 with the carbonyl group. The N6–C11 bond appears longer than N7–C16 [1.394(13) *vs.* 1.373(11) Å] but no definite conclusion can be drawn in view of the large standard deviations. The ethoxycarbonyl groups are located on opposite faces of the hydrazide bridge; the N6-ethoxycarbonyl group resides in an *exo* position and the N7-ethoxycarbonyl group is *endo*. The torsion angle between them (C11–N6–N7–C16) is 104° which presumably minimises steric interactions between these bulky vicinal substituents. In the crystal the carbamate groups adopt a conformation about the N–CO_2 bonds that places both ethoxy groups outwards on the flanks of the molecule (see Fig. 1). However dynamic NMR studies indicate that in solution other conformations about the carbamate bonds,

Table 3 RHF/3-21G imaginary frequencies (cm^{-1}), eigenvalues and corresponding eigenvectors (*C*) associated with the unique negative eigenvalue, and selected geometrical parameters (*G*) for the transition structures **TS1**, **TS2**, and **TS3**

TS1			**TS2**			**TS3**		
Frequency	594.9i		Frequency	320.7i		Frequency	320.7i	
Eigenvalue	−0.0786		Eigenvalue	−0.0382		Eigenvalue	−0.0325	
	G	*C*		*G*	*C*		*G*	*C*
C2–C3	1.386	−0.114	C2–O10	1.310	0.139	C5–O8	2.264	0.573
C2–N7	2.241	0.564	O10–C5	2.378	−0.878	C1–N7	1.970	0.653
C3–C4	1.373	0.112	C2–N7	1.623	−0.213	C16–N7–N6	114.5	−0.137
C5–N6	1.966	0.684	C5–O10–C2	79.2	0.111	C2–C1–N7	86.0	−0.177
C2–N7–C16	95.6	−0.117	H5–C5–O10	115.2	−0.158	H1–C1–N7	96.0	−0.109
C5–O10–C2–C3	−21.2	0.220	O10–C2–N7–C16	−188.1	0.125	C4–C5–N6–N7	−31.8	0.222
C5–O10–C2–N7	71.9	0.123	H3–C3–C2–O10	−121.2	−0.149	N7–C5–N6–C11	−157.4	−0.188
C2–O10–C5–N6	−73.3	−0.122				C1–N7–N6–C5	−47.3	−0.106
C2–N7–N6–C11	−109.6	0.170				H3–C3–C2–C1	−159.5	0.133
C2–O10–C5–H5	−179.7	0.102				H4–C4–C5–N6	−134.3	−0.102

Table 4 Total (au) and relative energies (kcal mol^{-1}) for the stationary points of the domino reaction between furfural **1** and dimethyl azodicarboxylate **9**

	HF/3-21G		HF/6-31G*		B3LYP/6-31G*//HF/6-31G*	
	E	E_r [a]	*E*	E_r [a]	*E*	E_r [a]
1 + **9**	−899.516240	0.0	−904.606728	0.0	−909.699196	0.0
IN1	−899.579931	−40.0	−904.632786	−16.4	−909.711672	−7.8
IN2	−899.538156	−13.8	−904.613365	−4.2	−909.703860	−2.9
10	−899.624876	−68.2	−904.675715	−43.3	−909.752649	−33.5
TS1	−899.496387	12.5	−904.557022	31.2	−909.681460	11.1
TS2	−899.511428	3.0	−904.578331	17.8	−909.680047	12.0
TS3	−899.532132	−10.0	−904.595479	7.1	−909.699384	−0.1

[a] Energies relative to **1** + **9**.

with one or both ethoxy groups directed inwards, are also significantly populated (see below).

The mechanism of adduct formation

It is known that substituted furans with electron-withdrawing groups are poor dienes in Diels–Alder cycloadditions,[4] however DEAZD is a very reactive dienophile. In a previous publication[1] we tentatively suggested that the bicyclo[3.2.1]-adduct **2** from furfural and DEAZD could have been formed in a domino process involving an initial Diels–Alder cycloaddition followed by a retro-1,3-dipolar cycloreversion to an azomethine imine and then a 1,3-dipolar cycloaddition (Scheme 2). In view of the fact that 2-acetylfuran gives a similar cycloadduct **7**, the molecular mechanism for these domino reactions has been investigated using *ab initio* MO methods[7] (see Experimental section on computing methods). In order to minimise computational times, the calculations were performed on the domino reaction between furfural **1** and dimethyl azodicarboxylate **9**. An extensive exploration of the potential energy surface for this domino process has rendered two intermediates, **IN1** and **IN2**, and three transition structures, **TS1**, **TS2** and **TS3**, corresponding with a three step mechanism (see Scheme 4). Table 3 shows the results of the geometries and the transition vectors (TV) for **TS1**, **TS2** and **TS3**, while Fig. 2 shows the geometries of the transition structures involved in this domino reaction. Table 4 lists the total and relative energies obtained at different levels of calculations, while Fig. 3 shows a schematic representation of the B3LYP/6-31G*//HF/6-31G* energy profiles[8] for the domino reaction between **1** and **9**.

The transition structure **TS1** corresponds to an asynchronous concerted [4 + 2] cycloaddition between furfural and dimethyl azodicarboxylate, where the lengths of the C2–N7 and C5–N6 forming bonds are 2.241 (2.228) and 1.966 (1.886) Å, respectively. (Values in parentheses correspond to 6-31G* geometries.) For the **TS1** the dominant components of TV are

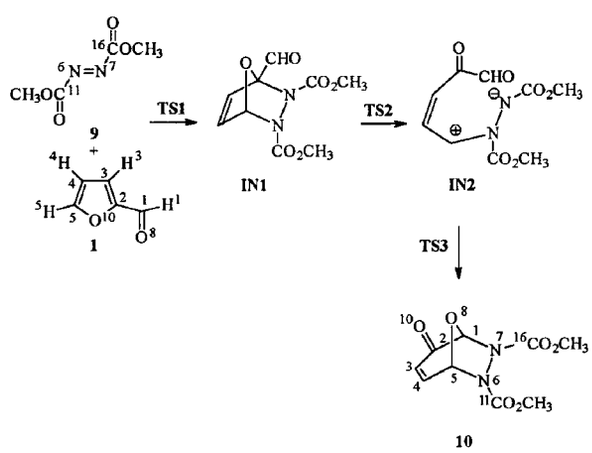

Scheme 4

associated with the C2–N7 and C5–N6 variables (the values are 0.564 and 0.684 respectively), and along with the other secondary variables present a TV similar to related concerted Diels–Alder cycloadditions. The potential energy barrier associated with **TS1** is 11.1 kcal mol^{-1} (relative energies corresponding to B3LYP/6-31G* single point calculations). Five-membered heterocycles such as pyrrole and furan act as electron-rich dienes in [4 + 2] cycloadditions with electron-withdrawing substituted dienophiles.[9] A Mulliken analysis of **TS1** shows a negative charge transfer (0.3 au) from furfural to dimethyl azodicarboxylate, indicating that furfural acts as an electron-rich diene despite the presence of the formyl group. This analysis also shows minimal charge variation at the formyl group on going from furfural to **TS1**, indicating that from an electronic standpoint this group does not take part in this cycloaddition. In practice, the free energy of activation ($\Delta G^{\ddagger}$) for the cycloaddition of **1** with **9** will be considerably greater than the calcu-

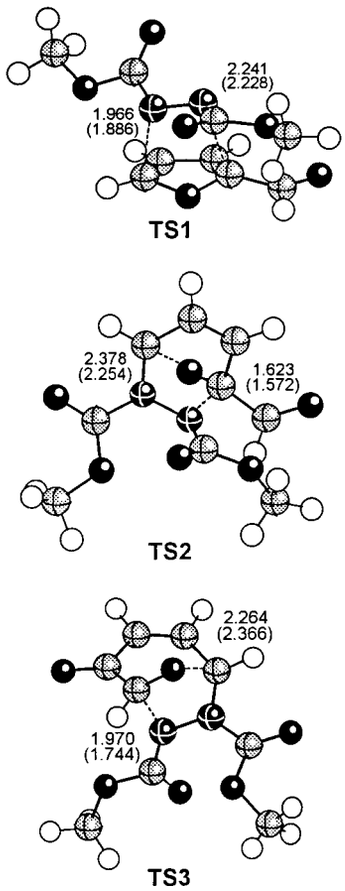

Fig. 2 Geometries of the transition structures corresponding to the domino reaction between furfural **1** and dimethyl azodicarboxylate **9**. The values given are the lengths of the bonds (Å) directly involved in the domino reaction calculated at the RHF/3-21G (RHF/6-31G*) levels.

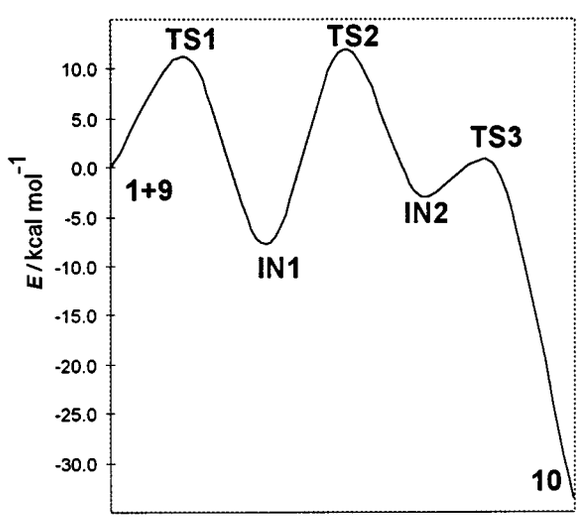

Fig. 3 Schematic representation of the energy profile for the domino reaction between **1** and **9**.

lated potential energy barrier of 11.1 kcal mol^{-1} as [4 + 2] cycloadditions have a large negative entropy of activation, typically in the range −30 to −40 cal mol^{-1} K^{-1} for additions involving a five-membered ring diene.[10] This would add 10–14 kcal mol^{-1} ($T\Delta S^{\ddagger}$) at 70 °C to the calculated potential energy barrier.

This [4 + 2] cycloaddition is less exothermic (−7.8 kcal mol^{-1}) than the usual Diels–Alder cycloadditions (for butadiene + ethene ΔH° is −40 kcal mol^{-1})[10] due to the loss of the aromaticity of the furan ring. Hence this process is reversible with a retro-Diels–Alder energy barrier of 19.0 kcal mol^{-1}. All attempts to find a stepwise mechanism through a zwitterionic intermediate for this cycloaddition have been unsuccessful, indicating that the first step of the reaction takes place through the concerted transition state **TS1**.

The isomerization of the intermediate **IN1** to the product **10** demands a two-bond breaking process to give the intermediate **IN2**, followed by a two-bond forming process to give the final product **10**. As in the first [4 + 2] cycloaddition, attempts to find a stepwise mechanism for the cleavage of **IN1** have been unsuccessful. Thus, the cleavage of the intermediate **IN1** takes place *via* the transition structure **TS2** which corresponds to a concerted bond breaking process. The barrier of 19.9 kcal mol^{-1} associated with **TS2** is very similar to the the retro-Diels–Alder reaction of intermediate **IN1**. At transition state **TS2**, the lengths of the O10–C5 and C2–N7 breaking bonds are 2.378 (2.254) and 1.623 (1.572) Å, respectively. These values indicate that this concerted process is asynchronous, the O10–C5 bond breaking process being more advanced than C2–N7 bond breaking. For **TS2** the dominant components of TV are associated with the O10–C5 and C2–N7 variables (the values are −0.878 and −0.213, respectively). The component associated with the O10–C2 variable shows that the bond order between the O10–C2 atoms changes from one to two. Finally, the component associated with the O10–C5–H5 variable is related to the change of hybridization at C5 from sp^3 to sp^2. The concerted nature of this process allows the delocalization of the negative charge that is developing at O10 onto C2 and N7 during the O10–C5 bond breaking process. This fact allows us to explain why a stepwise mechanism is not found for this cleavage process, since the bond breaking process of only one of the two bonds is very energetic.

The intermediate **IN2** is a zwitterionic species where the positive charge is principally located on C5, while the negative charge is located on N7. The process **IN1**→**IN2** is slightly endothermic (4.9 kcal mol^{-1}). The carbocationic C5 centre in **IN2** is stabilized by the conjugated C3–C4 double bond, and mainly by delocalization of the N6 lone pair. Thus the values of the C5–N6 bond length in **IN1** and **IN2** are 1.410 (1.487) and 1.375 (1.276) Å, respectively. The shorter C5–N6 bond length in **IN2** is in agreement with this delocalization. The negative charge located on N7 is stabilized by delocalization onto the attached carboxylate group.

This cleavage process is reversible, allowing a ring closure of intermediate **IN2** to give intermediate **IN1**. However, easy rotation around the C2–C3 bond allows the conversion of the intermediate **IN2** to the product **10** *via* the transition structure **TS3**. The potential barrier associated with this transition is very low (2.8 kcal mol^{-1}), though the free energy barrier will be somewhat higher due to unfavourable entropy factors. The process corresponds to the concerted formation of the C1–N7 and C5–O8 bonds. The lengths of these forming bonds are 1.970 (1.744) and 2.264 (2.366) Å respectively. In this transition structure C1–N7 bond formation is more advanced than C5–O8 bond formation, and the process can be considered as a nucleophilic attack of the anionic N7 atom on C1 of the formyl group. This process is favoured by the simultaneous attack of the negative charge that is developing at O8 on the carbocationic C5 centre. For the **TS3** the dominant components of TV are associated with the C5–O8 and C1–N7 variables (0.573 and 0.653 respectively) showing a more concerted process than for **TS2**. The components corresponding with the C2–C1–N7 and H1–C1–N7 variables are associated with the change of hybridization on C1 from sp^2 to sp^3, while the component corresponding with the C4–C5–N6–N7 variable is associated with the change of hybridization on C5 from sp^3 to sp^2.

The transition structure **TS3** is less energetic than **TS2** by 12.1 kcal mol^{-1} and consequently the transformation of the intermediate **IN2** into the product **10** is energetically favourable and highly exothermic (−30.6 kcal mol^{-1}). This determines that the process is irreversible. Both kinetic and thermodynamic

Table 5 Dynamic ^{1}H and ^{13}C NMR data for the two stereodynamic processes in cycloadduct **7**[a]

Signal analysed	δ	Conformer ratio[b]	$\Delta\nu$/Hz	J/Hz	Temperature[c]/°C	k[d]/s^{-1}	$\Delta G^{\ddagger}$[d]/kcal mol^{-1}
CH_3CH_2	1.21	1.0:0.86	11.7	7.1	−18.0	29.5[e]	13.14
C4	142.5	1.0:0.86	26.7	0	−13.0	46.8[e]	13.17
C5-H	6.39	1.0:0.88	25.6, 14.7	4.0	−70.5	40.9[e]	10.21
CO_2	157.8	1.0:0.9	109	0	−57.0	242[f]	10.2

[a] Determined in CD_2Cl_2 solution at 270.0 MHz (^{1}H) or 67.8 MHz (^{13}C). [b] Measured from low temperature spectra and adjusted slightly to optimise the fit between calculated and experimental lineshapes. [c] Temperature at which k was determined (at or close to the coalescence temperature). [d] Rate constants and $\Delta G^{\ddagger}$ given are for the minor→major process; $\Delta G^{\ddagger}$ for the major→minor process is 0.07 kcal mol^{-1} higher. [e] Determined by computer aided lineshape analysis. [f] Determined from the equation $k = \pi\Delta\nu/\sqrt{2}$.

controls favour this domino process to give the diazaoxabicyclooctenone **10**. Two structural features are responsible for the higher stability of the product **10** relative to the initial cycloadduct **IN1**. Firstly, expansion of the bicyclic system from [2.2.1] to [3.2.1] relieves strain (strain is high in the intermediate **IN1** due to the presence of the C3–C4 double bond in the bicyclic system). Secondly, the final system **10** is electronically stabilized due to the formation of an α,β-unsaturated ketone.

The 3-21G vibrational analysis gives the following imaginary frequencies for **TS1**, **TS2** and **TS3**: 594.9i, 320.9i and 320.7i cm^{-1}, respectively. These relatively low values indicate that these stationary points are associated with heavy atom motions, and for the **TS1** this imaginary value is similar to those found for related Diels–Alder cycloadditions. Moreover, the identical vibrational frequencies and negative eigenvalues found for **TS2** and **TS3** indicate that these transition structures are associated with similar heavy atom motions.

Variable temperature dynamic NMR studies

The ^{1}H and ^{13}C NMR spectra of compound **7** recorded at ambient temperature showed only one set of sharp well-resolved signals. Thus there was no evidence in the spectra of compound **7** for the dynamic broadening process previously observed for compound **2** in the temperature range 0 to 50 °C which was tentatively assigned to a bridge inversion process. This process may well be occurring in **7**, but we presume that the small relative population of the minor component in **2** (*ca.* 10%) is further reduced in adduct **7** to the extent that no dynamic exchange effects are evident in the NMR spectra. On lowering the temperature below 0 °C (CD_2Cl_2 solution) several of the signals in the ^{1}H NMR spectrum began to broaden and collapse. By −40 °C the upfield methyl triplet, downfield OCH_2 quartet, and the three ring signals C3-H, C4-H and C5-H had all split into two well resolved components with similar multiplicities and intensity ratios of *ca.* 0.9:1.0.

Similar effects were observed in the ^{13}C NMR over the same temperature range and by −40 °C most of the signals (except for the downfield OCH_2 at δ 64.5 and the ester C=O at δ 158.0) had split into two components with relative intensity *ca.* 0.85:1.0. A second dynamic exchange process was evident in NMR spectra recorded below −60 °C in CD_2Cl_2 solution. In the ^{1}H spectra, the signals from C5-H (δ 6.3) and the lower field methyl triplet (δ 1.3) broadened and at −96 °C had separated into two further components with an intensity ratio *ca.* 0.9:1.0. Similarly, in the ^{13}C NMR spectra recorded below −60 °C, the signals from C5 (δ 84.5), C1 (δ 94.7), C3 (δ 127.2), C4 (δ 142.5) and the three carbonyl groups broadened and resolved into two new components at −90 °C.

The rate constants and free energies of activation for both these processes, determined by analysis of the lineshape in the region of maximum exchange broadening, are given in Table 5. Each process was analysed from both the ^{1}H and ^{13}C lineshapes of the coalescing signals with the largest splittings to ensure optimum accuracy. A representative spectrum at coalescence is shown in Fig. 4. The resulting $\Delta G^{\ddagger}$ values are in excellent agreement for the ^{1}H and ^{13}C measurements (Table 5).

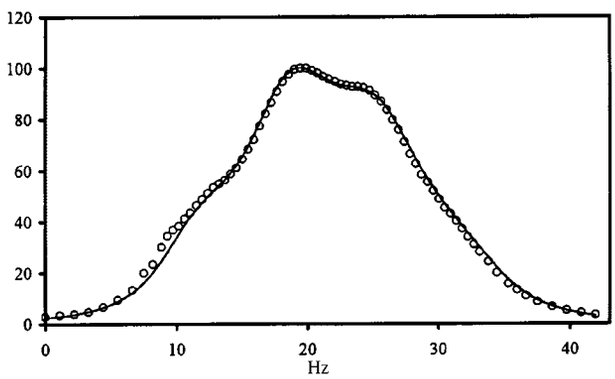

Fig. 4 Experimental (○) and best fit calculated (—) ^{1}H NMR lineshapes for the coalescing methyl triplets of **7** at −18.0 °C (k = 29.5 s^{-1}).

The barriers, coalescence temperatures and signal splitting patterns are very similar to those reported previously for processes 2 and 3 in cycloadduct **2** derived from furfural, leaving little doubt that they derive from the same stereodynamic processes. The process responsible for the coalescence between −10 and −20 °C can be assigned to rotation about one of the N–CO_2Et bonds as a barrier of 13.1 kcal mol^{-1} is in the expected range for this type of process based on literature data for cyclic 1,2-dialkoxycarbonylhydrazides.[11,12] The barrier of only 10.2 kcal mol^{-1} for the lower temperature coalescence (−50 to −70 °C) might appear to be too low for rotation about the other nonequivalent N–CO_2Et bond in **7** as the lowest barrier previously reported for such a process in a 1,2-dialkoxycarbonylhydrazide is 12.6 kcal mol^{-1}.[11,12] Accordingly, as previously suggested for **2**, this stereodynamic process could be associated with a process involving interchange of the two CO_2Et groups between *exo* and *endo* positions in adduct **7** by a combination of bridge twisting and nitrogen inversion. However, in view of the unusually high degree of pyramidality of N6 revealed by the X-ray crystal structure (ΣN6 = 333°) it is possible that the N6–CO rotational barrier could be abnormally low, conceivably as low as 10.2 kcal mol^{-1}. Thus the lone pair electrons on N6 would have more s-character due to the pyramidal geometry, leading to a weaker π-interaction with the carbonyl group and a lower rotational barrier. The stereodynamic process observed at *ca.* −15 °C, with $\Delta G^{\ddagger}$ = 13.1 kcal mol^{-1}, can then be assigned to rotation about the N7–CO bond. Nitrogen N7 is close to planarity as in acyclic 1,2-dialkoxycarbonylhydrazides, hence the N7–CO rotational barrier is in the normal range for this process.[11,12] On this basis the high temperature process previously observed[1] in the NMR spectra of the furfural adduct **2** ($\Delta G^{\ddagger}$ = 15.2 kcal mol^{-1}) would be reassigned to a combined bridge inversion–nitrogen inversion process.

Experimental

General procedures

Melting points were determined with a Kofler hot-stage apparatus and are uncorrected. ^{1}H NMR and ^{13}C NMR spectra were

recorded on Bruker AC-200, Bruker AC-250, Varian Gemini-300 and Jeol GSX-270 spectrometers. Chemical shifts are given in ppm. Mass spectra were obtained on a Hewlett-Packard 5930A spectrometer and high-resolution mass spectra were obtained using a VG Autospec, TRIO 1000 instrument. The ionization mode used in mass spectra was electron impact (EI) at 70 eV or chemical ionization (CI).

6,7-Diethoxycarbonyl-1-methyl-6,7-diaza-8-oxabicyclo[3.2.1]-oct-3-en-2-one (7)

The title compound (0.80 g, 35%) was obtained by heating 2-acetylfuran **6a** (0.90 g, 0.008 mol), DEAZD (4.28 g, 0.024 mol) and chloroform (16 ml) in a sealed tube at 70 °C for 9 days; mp 63–65 °C (from aqueous methanol); δ_H (250 MHz; $CDCl_3$) 1.22 (3H, t, *J* 7 Hz), 1.33 (3H, t, *J* 7 Hz), 1.76 (3H, s), 4.16 (2H, q, *J* 7 Hz), 4.31 (2H, q, *J* 7 Hz), 6.05 (1H, d, *J* 9.8 Hz), 6.27 (1H, d, *J* 4 Hz) and 7.02 (1H, dd, *J* 9.8 and 4 Hz); δ_C (62.9 MHz; $CDCl_3$) 14.0 (q), 14.1 (q), 16.6 (q), 62.8 (t), 63.9 (t), 84.0 (d), 94.7 (s), 127.0 (d), 141.4 (d), 155.0 (s), 157.3 (s) and 188.9 (s) (Found: C, 50.88; H, 5.61; N, 9.79; M^+ 284.1008. $C_{12}H_{16}N_2O_6$ requires C, 50.70; H, 5.67; N, 9.85; M 284.1008).

Diethyl 1-[(5-methyl-2-furyl)carbonyl]hydrazine-1,2-dicarboxylate (8)

The title compound was obtained as an oil (0.78 g, 12%) by heating 2-formyl-5-methylfuran **6b**, (2.5 g, 0.022 mol), DEAZD (3.83 g, 0.022 mol) and dichloromethane (20 ml) in a sealed tube at 100 °C for 30 h; δ_H(250 MHz; $CDCl_3$) 1.19 (6H, m), 2.28 (3H, s), 4.12 (4H, m), 6.07 (1H, d, *J* 3.3 Hz), 7.08 (1H, d, *J* 3.3 Hz) and 7.63 (1H, br s); δ_C (62.9 MHz; $CDCl_3$) 13.6 (q), 13.7 (q), 14.0 (q), 62.2 (t), 63.7 (t), 108.7 (d), 121.4 (d), 144.4 (s), 153.2 (s), 155.2 (s), 155.6 (s) and 157.4 (s) (Found: MH^+ [CI] 285.1088. $C_{12}H_{17}N_2O_6$ requires MH 285.1087).

X-Ray crystallographic data

Crystals of **7** are orthorhombic, space group $P2_12_12_1$, $C_{12}H_{16}N_2O_4$, $M = 284.27$, $Z = 4$, $a = 7.784(1)$, $b = 8.311(1)$ and $c = 22.615(1)$ Å, $V = 1463.0(3)$ Å^3, $F(000) = 600$, μ(Mo-Kα) = 0.10 mm^{-1}, $R(F_o) = 0.073$ for 823 observed reflections with $I > 2\sigma(I)$, $wR_2(F^2) = 0.217$ for all 944 unique reflections. Data in the θ range 2–20° were collected on a Nonius MACH3 diffractometer using monochromatic Mo-Kα radiation and corrected for Lorentz and polarisation effects. The structure was solved by direct methods and refined by full-matrix least-squares using SHELXL-93[13] and all F^2 data. Due to the poor scattering ability of the crystal and the subsequent decomposition during data collection, all non-H atoms were allowed only isotropic motion. The H atoms were placed in calculated positions and allowed to ride on the parent atom.[14] The absolute structure could not be determined reliably; both the Flack parameter test and an *R*-factor test were inconclusive. Full details of molecular dimensions, fractional co-ordinates, thermal parameters and structure factor listings are available from the authors.‡

Computing methods

All gas phase calculations have been carried out with the GAUSSIAN94 suite of programs.[15] An extensive characterization of the potential energy surface has been performed at HF/3-21G level to ensure that all relevant stationary points have been located and properly characterized. The stationary points were characterized by frequency calculations in order to verify that transition structures have one and only one imaginary frequency. The HF/3-21G frequencies were used as an initial guess in the search of the HF/6-31G*[7] structures. The optimizations were carried out using the Berny analytical gradient optimization method.[16] The transition vectors, which yields very concisely the essentials of the chemical process under study,[17] have been characterized. Finally, accurate barrier heights have been obtained by means of B3LYP/6-31G*[8] single point energy calculations, which have been shown to be in quite reasonable agreement with experimental activation energy values.[18] DFT calculations using the B3LYP hybrid function have been shown to be in good agreement with experimental activation energy values.[19] The presence of two flexible ester groups in this system means that it is very computationally expensive to fully optimize the structures, so B3LYP/6-31G*//HF/6-31G* calculations were used to obtain more accurate relative energies.

Dynamic NMR studies

Variable temperature ^{1}H and ^{13}C NMR spectra were recorded on a Jeol GSX-270 spectrometer operating at 270 and 67.8 MHz respectively. Probe temperatures were measured to ±0.1 °C using a Comark Model C9001 digital thermometer equipped with a copper-constantan fine gauge thermocouple lead inserted into a non-spinning sample tube containing 0.7 ml of dichloromethane. Exchange broadened spectra were analysed using a PC version of the iterative multisite exchange program INMR.[20] Component lines of first-order spin coupled multiplets in ^{1}H spectra were treated as separate sites with the appropriate relative intensity. Thus the coalescence of the methyl triplet signals at −18.0 °C was treated as a six-site exchange system and the coalescence of the two C5–H doublet of doublets at −70.5 °C was analysed as an eight-site system.

Acknowledgements

We thank the Mº Education y Ciencia (project PB95-1076) and the Universitate de Valencia (project UV97-2219) for financial support, and the Cork University Foundation for funding the purchase of the X-ray diffractometer.

References

1 E. Zaballos-Garcia, M. E. Gonzalez-Rosende, J. M. Jorda-Gregori, J. Sepúlveda-Arques, W. B. Jennings, D. O'Leary and S. Twomey, *Tetrahedron*, 1997, **53**, 9313.
2 M. E. Gonzalez-Rosende, O. Lozano-Lucia, E. Zaballos-Garcia and J. Sepúlveda-Arques, *J. Chem. Res.* (*S*), 1995, 260.
3 A. R. Katritsky, C. W. Rees and E. F. V. Scriven, eds., *Comprehensive Heterocyclic Chemistry*, Pergamon Press, vol. II, 1996.
4 A. Padwa, M. Dimitroff, A. G. Waterson and T. Wu, *J. Org. Chem.*, 1997, **62**, 4088; K. T. Potts and E. B. Walsh, *J. Org. Chem.*, 1988, **53**, 1199; J. A. Moore and E. M. Partain III, *J. Org. Chem.*, 1983, **48**, 1105; W. B. Dauben and H. O. Krabbenhoft, *J. Am. Chem. Soc.*, 1976, **98**, 1992; W. L. Nelson and D. R. Allen, *J. Heterocycl. Chem.*, 1972, **9**, 561.
5 G. Desimoni and G. Tacconi, *Chem. Rev.*, 1975, **75**, 651.
6 K. H. Linke and H. G. Kalker, *Z. Anorg. Allg. Chem.*, 1977, **434**, 165; G. Reck, M. Just and R. Koch, *Cryst. Res. Technol.*, 1987, **22**, 395; N. G. Anderson, D. A. Lust, K. A. Colapret, J. H. Simpson, M. F. Malley and J. Z. Gougoutas, *J. Org. Chem.*, 1996, **61**, 7955; M. Kaftory, T. H. Fisher and S. M. Dershem, *J. Chem. Soc., Perkin Trans. 2*, 1989, 1887; J. Barluenga, F. J. Gonzalez, S. Fustero, M. de la C. Foces-Foces, F.-H. Cano and A. S. Feliciano, *J. Chem. Res.*, 1989, (*s*) 66; (*m*) 569.
7 W. J. Hehre, L. Random, P. V. R. Schleyer and J. A. Pople, *Ab initio Molecular Orbital Theory*, Wiley, New York, 1986.
8 C. Lee, W. Yang and R. G. Parr, *Phys. Rev. B*, 1988, **37**, 785; A. D. Becke, *J. Chem. Phys.*, 1993, **98**, 5648.
9 L. R. Domingo, M. Arnó and J. Andrés, *J. Am. Chem. Soc.*, 1998, **120**, 1617; L. R. Domingo, M. T. Picher, M. Arnó, J. Andrés and V. S. Safont, *J. Mol. Struct. (Theochem)*, 1998, **426**, 257.

‡ Full crystallographic details, excluding structure factor tables, have been deposited at the Cambridge Crystallographic Data Centre (CCDC). For details of the deposition scheme see 'Instructions for Authors', *J. Chem. Soc., Perkin Trans. 2*, available *via* the RSC web page (http://www.rsc.org/authors). Any request to the CCDC for this material should quote the full literature citation and the reference number 188/147.

10 O. Diels and K. Alder, *Justus Liebigs Ann. Chem.*, 1928, **460**, 98; R. B. Woodward and R. Hoffmann, *Angew. Chem.*, *Int. Ed. Engl.*, 1969, **8**, 781; A. Wassermann, *Trans. Faraday Soc.*, 1938, **34**, 129.
11 J. E. Anderson and J. M. Lehn, *Tetrahedron*, 1968, **24**, 123.
12 For a review of hydrazide stereodynamics see: S. F. Nelsen, in *Acyclic Organonitrogen Stereodynamics*, J. B. Lambert and Y. Takeuchi, eds., VCH, 1992, p. 89.
13 G. M. Sheldrick, SHELX-97, Programs for the solution and refinement of crystal structures, University of Gottingen, Germany, 1997.
14 A. L. Spek, PLATON, Molecular Graphics Program, University of Utrecht, Holland, 1998.
15 GAUSSIAN94, Revision B.1, M. J. Frisch, G. W. Trucks, H. B. Schlegel, P. M. W. Gill, B. G. Johnson, M. A. Robb, J. R. Cheeseman, T. Keith, G. A. Petersson, J. A. Montgomery, K. Raghavachari, M. A. Al-Laham, V. G. Zakrzewski, J. V. Ortiz, J. B. Foresman, J. Cioslowski, B. B. Stefanov, A. Nanayakkara, M. Challacombe, C. Y. Peng, P. Y. Ayala, W. Chen, M. W. Wong, J. L. Andres, E. S. Replogle, R. Gomperts, R. L. Martin, D. J. Fox, J. S. Binkley, D. J. Defrees, J. Baker, J. P. Stewart, M. Head-Gordon, C. Gonzalez and J. A. Pople, Gaussian, Inc., Pittsburgh, PA, 1995.
16 H. B. Schlegel, *J. Comput. Chem.*, 1982, **3**, 214; H. B. Schlegel, "Geometry Optimization on Potential Energy Surface", in *Modern Electronic Structure Theory*, ed. D. R. Yarkony, World Scientific Publishing, Singapore, 1994.
17 J. W. McIver, Jr., *Acc. Chem. Res.*, 1974, **7**, 72.
18 B. Jursic and Z. Zdravkovski, *J. Chem. Soc.*, *Perkin Trans. 2*, 1995, 1223; B. Jursic, *J. Mol. Struct. (Theochem)*, 1996, **365**, 55; E. Goldstein, B. Beno and K. N. Houk, *J. Am. Chem. Soc.*, 1996, **118**, 6036.
19 L. R. Domingo, J. F. Sanz-Cervera, R. M. Williams, M. T. Picher and J. A. Marco, *J. Org. Chem.*, 1997, **62**, 1662; L. R. Domingo, M. T. Picher and R. J. Zaragozá, *J. Org. Chem.*, in the press.
20 W. B. Jennings, *J. Chem. Soc.*, *Chem. Commun.*, 1971, 867; J. Burdon, J. C. Hotchkiss and W. B. Jennings, *J. Chem. Soc.*, *Perkin Trans. 2*, 1976, 1052.

Paper 8/06628K